

## HISTO-ANATOMICAL INVESTIGATION ON *LYSIMACHIA PUNCTATA* L. (PRIMULACEAE) SPECIES

**BEJENARU L. E.<sup>1</sup>, BEJENARU CORNELIA<sup>2</sup>, MOGOȘANU G. D.<sup>1</sup>, OANCEA CARMEN NICOLETA<sup>2</sup>**

<sup>1</sup> Department of Pharmacognosy & Phytotherapy, Faculty of Pharmacy, University of Medicine and Pharmacy of Craiova, 2 Petru Rareș Street, 200349 Craiova.

<sup>2</sup> Department of Vegetal & Animal Biology, Faculty of Pharmacy, University of Medicine and Pharmacy of Craiova, 2 Petru Rareș Street, 200349 Craiova, e-mail: carmen2\_bejenaru@yahoo.com.

**Keywords:** *Lysimachia punctata* L., histo-anatomy, investigation

### ABSTRACT

*This paper presents the histo-anatomical investigation on the roots, rhizomes, aboveground stems and leaves of Lysimachia punctata species. In addition, the pharmacological importance of Lysimachia sp. is highlighted by modern and cutting-edge researches.*

### INTRODUCTION

*Lysimachia punctata* L., spotted (dotted) loosestrife, *Primulaceae* family, a perennial species of 50–100 cm tall, grows on riverbanks, swamps and scrubs. It is native to Central and Southern Europe and naturalized in Northern America (Ciocârlan, 2000).

Underground and aerial parts of *Lysimachia* species contain some active principles such as flavonoids (Tóth *et al.*, 2012; Sun *et al.*, 2013), polyphenolic acids (Tóth *et al.*, 2012), benzoquinone pigments (Podolak & Strzałka, 2008), essential oil (Dötterl & Schäffler, 2007; Liu *et al.*, 2012), saponosides (Podolak *et al.*, 2010; Koczurkiewicz *et al.*, 2013; Podolak *et al.*, 2013).

From the pharmacological point of view, the active principles of *Lysimachia* sp. exhibit some important actions: cytotoxic, apoptosis-inductive and antitumoral (Podolak *et al.*, 2005 & 2013; Liu *et al.*, 2010), attenuation of invasive potential of prostate cancer cells (Koczurkiewicz *et al.*, 2013), diuretic and kidney protective (Lien *et al.*, 2012), antioxidant (Wei *et al.*, 2012), anti-inflammatory (Zhang *et al.*, 2002), vasorelaxant *via* endothelium-dependent mechanism (Lee *et al.*, 2010a), antithrombotic (Lee *et al.*, 2010b), vermifuge (Challam *et al.*, 2010), anticholecystitis, cholagogue and hepatoprotective (Yang *et al.*, 2011; Wang *et al.*, 2012), inhibition of adipocyte differentiation and obesity induced by high-fat diet (Seo *et al.*, 2012).

In the specialty papers, there are scarce and incomplete data concerning *L. punctata* histo-anatomy (Shao *et al.*, 2007). The aim of our paper was the histo-anatomical investigation of the above-mentioned species taking into account its medicinal importance.

### MATERIAL AND METHODS

The vegetal material was harvested from *L. punctata* plants in blossom, in June 2013, from the surroundings of Orșova City, Mehedinți County, Romania.

The fixation and preservation of roots, rhizomes, aboveground stems and leaves were achieved in 70% alcohol. The cross-sections were obtained using botanical razor.

After washing with distilled water, the cross-sections were clarified using 10% sodium hypochlorite (Javel water). Then, the clarifying agent was removed by washing with distilled water. Congo red–chrysoidine mixture was used for the staining of cross-sections. Depending on the chemical composition of cell membranes, the reactive induced various stains: pink to red for cellulose, yellow for suberin, brown for lignified membranes (Andrei & Paraschivoiu, 2003).

Stained and mounted cross-sections were analyzed on a Krüss binocular photon microscope at diverse objectives (×4, ×10, ×40) and then photographed on a Soligor SR 300

system adapted to the microscope.

According to some classical authors (Toma & Rugină, 1998), the description of microscopic cross-sections was accomplished.

The assessment of stomatal index was made using  $\times 40$  objective (corresponding on  $0.037 \text{ mm}^2$  area) on a Nikon Eclipse 55i binocular photon microscope coupled with a Nikon DS-Fi1 high definition video camera. Image acquisition and processing were performed using ImageProPlus ver. 6.0 software package. For each bottom, middle and upper area of the examined leaf's limb, the average of 10 analyses were taken into consideration.

## RESULTS AND DISCUSSIONS

### Structure of root

The root has sinuous round shape and primary structure. From the outside to the inside of the cross-section, the following tissue sequence was noticed:

A single layer of small prosenchymatous cells with numerous absorptive hairs made the rhizodermis.

A single layer of small heterodiametric cells with suberin-impregnated walls forms the exodermis.

The cortical parenchyma is well differentiated, with many reserve substances. It is made by 10–15 layers of small heterodiametric cells delineating small intercellular spaces.

A single layer of endodermis circumscribes the inner part of primary cortex.

The central cylinder is protected by a single cellulosic pericycle layer. The simple xylem and phloem conducting fascicles (8–10) are alternately disposed and separated by cellulosic medullary rays.

The medullary parenchyma is of meatus-type (Figures 1 and 2).



Figure 1. Cross-section through *L. punctata* root. Congo red–chrysoidine staining,  $\times 100$ .

1 – Rhizodermis, 2 – Exodermis, 3 – Cortical parenchyma, 4 – Endodermis,  
5 – Pericycle, 6 – Xylem fascicle, 7 – Phloem fascicle,  
8 – Medullary parenchyma.

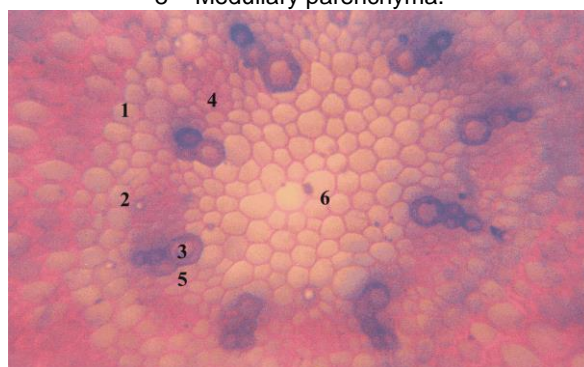


Figure 2. Cross-section through *L. punctata* root. Congo red–chrysoidine staining,  $\times 400$ .

1 – Endodermis, 2 – Pericycle, 3 – Xylem fascicle, 4 – Phloem fascicle, 5 – Medullary ray, 6 – Medullary parenchyma.

### Structure of rhizome

The rhizome shows sinuous round shape and secondary structure because of libero-ligneous cambium. In cross-section, from the outside to the inside, the following histological sequence is remarked (Figure 3):

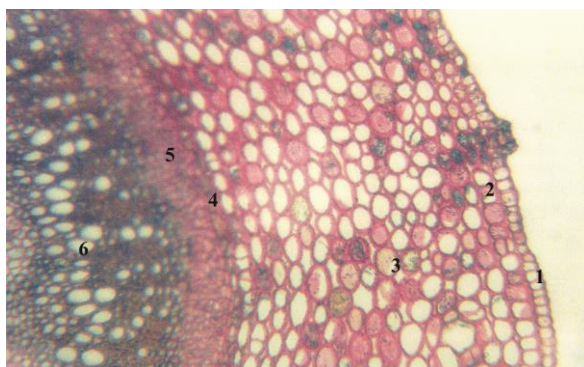


Figure 3. Cross-section through *L. punctata* rhizome. Congo red–chrysoidine staining,  $\times 100$ . 1 – Epidermis, 2 – Hypodermis, 3 – Cortical parenchyma, 4 – Endodermis, 5 – Phloem tissue, 6 – Xylem tissue.

The epidermis is made of a single layer of isodiametric cells, with thickened external and internal tangential walls and thin radial walls. Tangential external walls are bulged and covered by a thin cuticle.

The bark is constituted of a single layer of hypodermis, with small cells, nearly isodiametric, uniformly disposed and alternative with epidermal cells. The cortical parenchyma is well represented by 15–17 meatus-type cellular layers with reserve substances. To the inner part of the cross-section, a single layer of endodermis with Caspary's thickenings on the lateral walls bound the bark.

Generated by the libero-ligneous cambium, the conducting tissues are predominantly secondary and arranged in two concentric rings. The phloem tissue forms a thin ring to the outside, being made by sieve tubes, annex cells and phloem parenchyma. Medullary rays are pluricellular, uniseriate, cellulosic. The xylem tissue forms a thick ring to the inside, being made by big caliber secondary xylem vessels uniformly dispersed in the libriform tissue mass. Medullary rays are pluricellular, uniseriate, lignified. The primary vessels have small diameter and are accompanied by xylem parenchyma.

Meatus-type medullary parenchyma occupies the rhizome's center (Figures 4–6).

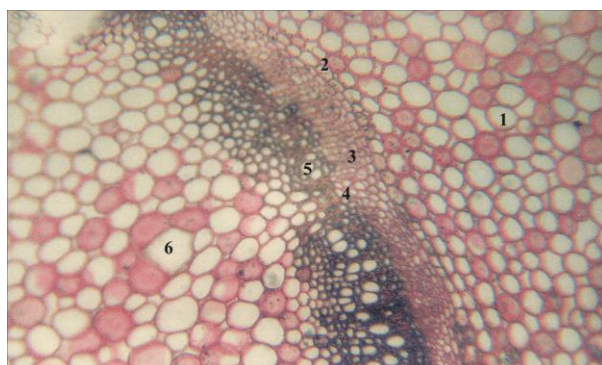


Figure 4. Cross-section through *L. punctata* rhizome. Congo red–chrysoidine staining,  $\times 100$ . 1 – Cortical parenchyma, 2 – Endodermis, 3 – Phloem tissue, 4 – Libero-ligneous cambium, 5 – Xylem tissue, 6 – Medullary parenchyma.

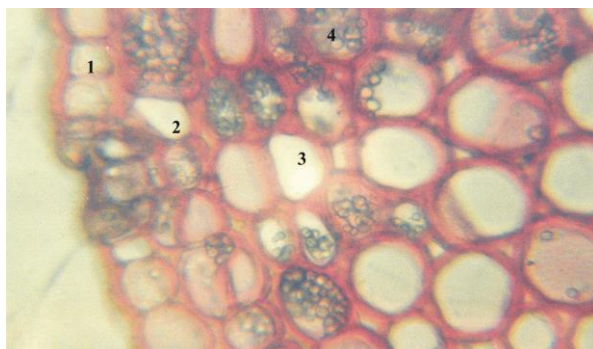


Figure 5. Cross-section through *L. punctata* rhizome. Congo red–chrysoidine staining, ×400. 1 – Epidermis, 2 – Hypodermis, 3 – Cortical parenchyma, 4 – Reserve substances.

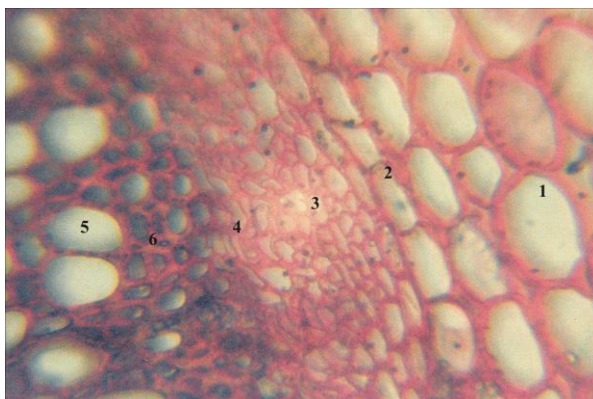


Figure 6. Cross-section through *L. punctata* rhizome. Congo red–chrysoidine staining, ×400. 1 – Cortical parenchyma, 2 – Endodermis, 3 – Phloem tissue, 4 – Libero-ligneous cambium, 5 – Secondary xylem vessel, 6 – Libriform tissue.

### Structure of aboveground stem

The aboveground stem has four-rib round shape and secondary structure. In cross-section, from the outside to the inside, the following tissue sequence was found:

The epidermis is made of a single layer of flattened small cells, with thickened external and internal tangential walls and thin radial walls. Here and there, pluricellular uniseriate or bicellular tector hairs and glandular hairs are observed.

The angular collenchyma is well represented at the four ribs level.

The cortical parenchyma is from meatus-type with periphloemic sclerenchyma caps to the inner part.

The conducting tissues are predominantly secondary and organized in two concentric circles.

The phloem tissue is poorly developed, including sieve tubes, few annex cells and phloem parenchyma. Medullary rays are pluricellular, uniseriate, cellulosic.

Developed by libero-ligneous cambium, the secondary xylem tissue is well represented by big caliber secondary xylem vessels arranged in radial rows in the libriform tissue mass. The primary vessels are few and accompanied by xylem parenchyma. Medullary rays are pluricellular, uniseriate, lignified. In longitudinal radial section, the xylem vessels show reticular, curly and spiral thickenings.

Meatus-type medullary parenchyma is well represented into the central part of the aboveground stem (Figures 7–10).



Figure 7. Cross-section through *L. punctata* aboveground stem. Congo red–chrysoidine staining, ×40. Overview.

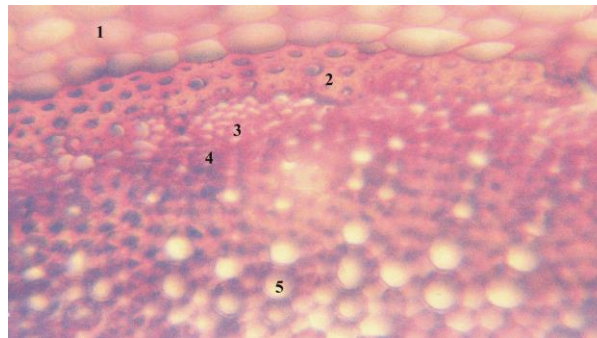


Figure 8. Cross-section through *L. punctata* aboveground stem. Congo red–chrysoidine staining, ×400. 1 – Cortical parenchyma, 2 – Sclerenchyma cap, 3 – Phloem tissue, 4 – Libero-ligneous cambium, 5 – Secondary xylem vessel.

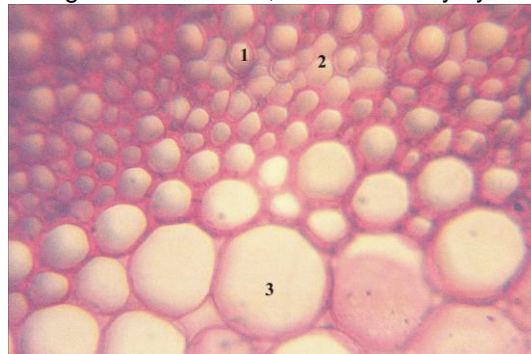


Figure 9. Cross-section through *L. punctata* aboveground stem. Congo red–chrysoidine staining, ×400. 1 – Primary xylem vessel, 2 – Xylem parenchyma, 3 – Medullary parenchyma.

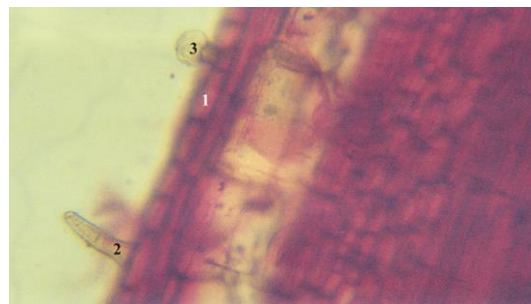


Figure 10. Longitudinal radial section through *L. punctata* aboveground stem. Congo red–chrysoidine staining, ×400. 1 – Epidermis, 2 – Bicellular tector hair, 3 – Glandular hair.

### Structure of leaf's limb

In cross-section, the leaf's limb shows the following histological order:

The upper epidermis is made of a single layer of heterodiametric big cells, with thickened external and internal tangential walls and thin radial walls. The external walls are bulged and covered by a thick cuticle. From point to point, anomocytic stomata, bi- and pluricellular uniseriate tector hairs are found.

The mesophyll is made of a single layer of palisade tissue to the ventral side and 3–4 layers of lacunose parenchyma to the dorsal side. The palisade cells are tall, leaving small intercellular spaces. The lacunose parenchyma cells are small, irregular in shape, leaving big aeriferous spaces. Into the leaf's mesophyll, collateral libero-ligneous fascicles are found.

The lower epidermis is made of a single layer of smaller cells compared to the upper epidermis. The lower epidermal cells have thickened external and internal tangential walls, and thin radial walls. Here and there, anomocytic stomata, long uniseriated pluricellular tector hairs and bicellular glandular hairs are exhibited.

The leaf's limb has bifacial dorsiventral structure from amphistomatic type. Through the separation of both upper and lower epidermis, anomocytic stomata are found.

In cross-section, the median rib is prominent to the dorsal side. At the ribs' level, a central big libero-ligneous conducting fascicle was found. The xylem tissue, located to the ventral side, is made of xylem vessels arranged in radial rows and separated by cellulosic medullary rays. The phloem tissue, located to the dorsal side of leaf's limb, is made of sieve tubes, annex cells and phloem parenchyma. At this level, the medullary rays are also cellulosic. At the median rib's level, the conducting fascicle is seated in a homogenous mass of fundamental parenchymatic tissue (Figures 11–13).

For *L. punctata* leaf's limb, our investigation shows a stomatal index of 21.4–21.8 (Figures 14 and 15).



Figure 11. Cross-section through *L. punctata* leaf's limb. Congo red–chrysoidine staining,  $\times 400$ . 1 – Upper epidermis, 2 – Tector hair, 3 – Palisade parenchyma, 4 – Lacunose parenchyma, 5 – Lower epidermis.



Figure 12. Cross-section through *L. punctata* leaf's median rib. Congo red–chrysoidine staining,  $\times 400$ . 1 – Upper epidermis, 2 – Tector hair, 3 – Leaf parenchyma, 4 – Libero-ligneous conducting fascicle.

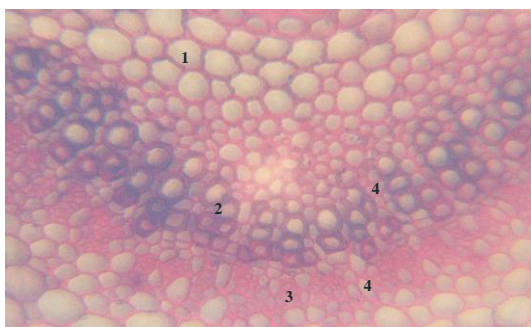


Figure 13. Cross-section through *L. punctata* leaf's median rib. Congo red–chrysoidine staining, ×400. 1 – Leaf parenchyma, 2 – Xylem tissue, 3 – Phloem tissue, 4 – Medullary ray.

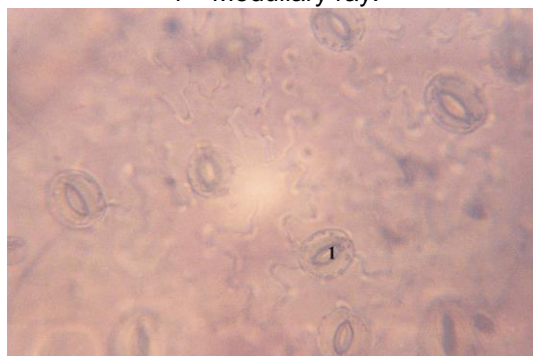


Figure 14. *L. punctata* upper epidermis. Congo red–chrysoidine staining, ×400. 1 – Anomocytic stomata.



Figure 15. *L. punctata* lower epidermis. Congo red–chrysoidine staining, ×400. 1 – Anomocytic stomata, 2 – Tector hair insertion.

### Structure of petiole

In cross-section, the petiole has a half-round shape and the following tissue sequence from outside to the inside (Figure 16):

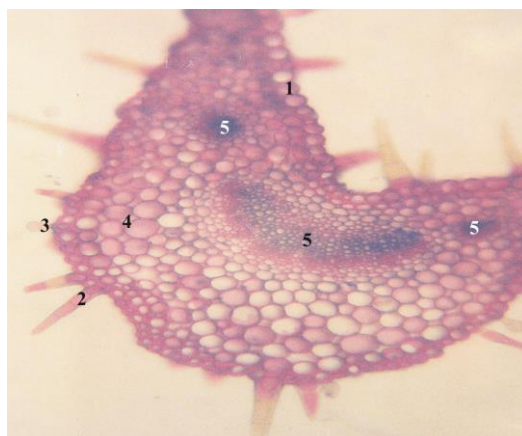


Figure 16. Cross-section through *L. punctata* petiole. Congo red–chrysoidine staining, ×100. 1 – Epidermis, 2 – Tector hair, 3 – Glandular hair, 4 – Fundamental parenchyma, 5 – Conducting fascicle.

A single layer of small cells with thickened internal and external tangential walls and thin radial walls makes the epidermis. At this level, many uniseriated bi- and pluricellular tector and glandular hairs are found.

Into the homogeneous fundamental meatus-type parenchyma, three libero-ligneous conducting tissues arranged on an arch are observed: a big one, half-round, centrally disposed fascicle and other two small fascicles.

## CONCLUSIONS

The histo-anatomical investigation on the vegetative organs of *L. punctata* species was accomplished. The root has sinuous round shape and primary structure. The rhizome shows sinuous round shape and secondary structure due to the libero-ligneous cambium. The aboveground stem is characterized by four-rib round shape, secondary structure and periphloemic sclerenchyma caps to the inner part of the cortical parenchyma. The leaf's limb has bifacial dorsiventral structure from amphistomatic type. Anomocytic stomata are found on both upper and lower epidermis. The petiole has a half-round shape and three libero-ligneous fascicles.

## BIBLIOGRAPHY

**Andrei M., Paraschivoiu Roxana Maria,** 2003, Microtehnică botanică. Edit. Niculescu, București, 222 pag.

**Challam M., Roy B. and Tandon V.,** 2010, Effect of *Lysimachia ramosa* (Primulaceae) on helminth parasites: motility, mortality and scanning electron microscopic observations on surface topography. Vet. Parasitol. 169(1–2): 214–218.

**Ciocârlan V,** 2000, Flora ilustrată a României. *Pteridophyta et Spermatophyta*, ediția a 2-a revizuită și adăugită. Edit. Ceres, București, 1138 pag.

**Dötterl S. and Schäffler I.,** 2007, Flower scent of floral oil-producing *Lysimachia punctata* as attractant for the oil-bee *Macropis fulvipes*. J. Chem. Ecol. 33(2): 441–445.

**Koczurkiewicz P., Podolak I., Skrzeczyńska-Moncznik J., Sarna M., Wójcik K. A., Ryszawy D., Galanty A., Lasota S., Madeja Z., Czyż J. and Michalik M.,** 2013, Triterpene saponosides from *Lysimachia ciliata* differentially attenuate invasive potential of prostate cancer cells. Chem. Biol. Interact. 206(1): 6–17.

**Lee J. O., Chang K., Kim C. Y., Jung S. H., Lee S. W. and Oak M. H.,** 2010a, *Lysimachia clethroides* extract promotes vascular relaxation via endothelium-dependent mechanism. J. Cardiovasc. Pharmacol. 55(5): 481–488.

**Lee J. O., Park D. H., Jung S. H., Lee S. W. and Oak M. H.,** 2010b, The antithrombotic activity of ethanol extract of *Lysimachia clethroides*. J. Korean Soc. Appl. Biol. Chem. 53(3): 384–387.

**Lien E. J. C., Lien L. L. M., Wang R. and Wang J.,** 2012, Phytochemical analysis of medicinal plants with kidney protective activities. Chin. J. Integr. Med. 18(10): 790–800.

**Liu R. L., Liu J. S., Lin Z. L., Jiang H. H. and Chen P. Z.,** 2012, GC-MS analysis of volatile oils extracted from *Lysimachia christinae* Hance by different methods. J. Med. Plant. 3(8): 38–40, 43.

**Liu Y. L., Tang L. H., Liang Z. Q., You B. G. and Yang S. L.,** 2010, Growth inhibitory and apoptosis inducing by effects of total flavonoids from *Lysimachia clethroides* Duby in human chronic myeloid leukemia K562 cells. J. Ethnopharmacol. 131(1): 1–9.

**Podolak I. and Strzałka M.,** 2008, Qualitative and quantitative LC profile of embelin and rapanone in selected *Lysimachia* species. Chromatographia. 67(5–6): 471–475.

**Podolak I., Galanty A. and Janeczko Z.,** 2005, Cytotoxic activity of embelin from *Lysimachia punctata*. Fitoterapia. 76(3–4): 333–335.

**Podolak I., Galanty A. and Sobolewska D.,** 2010, Saponins as cytotoxic agents: a review. Phytochem. Rev. 9(3): 425–474.

**Podolak I., Koczurkiewicz P., Galanty A. and Michalik M.,** 2013, Cytotoxic triterpene saponins from the underground parts of six *Lysimachia* L. species. Biochem. Syst. Ecol. 47: 116–120.

**Seo J. B., Park S. W., Choe S. S., Jeong H. W., Park J. Y., Choi E. W., Seen D. S., Jeong J. Y. and Lee T. G.,** 2012, Foenumoside B from *Lysimachia foenum-graecum* inhibits adipocyte differentiation and obesity induced by high-fat diet. Biochem. Biophys. Res. Commun. 417(2): 800–806.

**Shao J. W., Zhang X. P. and Zhu G. P.,** 2007, The microcharacteristics of leaf

surface and its systematic implication in *Lysimachia*. Bull. Bot. Res. 27(1): 43–49.

**Sun D., Dong L., Guo P., Shi X., Gao J., Ren Y., Jiang X., Li W., Wang C. and Wang Q.**, 2013, Simultaneous detection of flavonoids and phenolic acids in *Herba Lysimachiae* and *Herba Desmodii Styracifolii* using liquid chromatography tandem mass spectrometry. Food Chem. 138(1): 139–147.

**Toma C., Rugină Rodica**, 1998, Anatomia plantelor medicinale. Atlas. Edit. Academiei Române, București, 320 pag.

**Tóth A., Riethmüller E., Alberti Á., Végh K. and Kéry Á.**, 2012, Comparative phytochemical screening of phenoloids in *Lysimachia* species. Eur. Chem. Bull. 1(1–2): 27–30.

**Wang J., Zhang Y., Zhang Y., Cui Y., Liu J. and Zhang B.**, 2012, Protective effect of *Lysimachia christinae* against acute alcohol-induced liver injury in mice. Biosci. Trends. 6(2): 89–97.

**Wei J. F., Zhang Y. B. and Kang W. Y.**, 2012, Antioxidant and  $\alpha$ -glucosidase inhibitory compounds in *Lysimachia clethroides*. Afr. J. Pharm. Pharmacol. 6(46): 3230–3234.

**Yang X., Wang B. C., Zhang X., Liu W. Q., Qian J. Z., Li W., Deng J., Singh G. K. and Su H.**, 2011, Evaluation of *Lysimachia christinae* Hance extracts as anticholecystitis and cholagogic agents in animals. J. Ethnopharmacol. 137(1): 57–63.

**Zhang L., Meng J., Chen H. and Han X.**, 2002, The effects of *n*-butanol fraction of *Lysimachia hemsleyana* on the activities of lymphocytes in mice. Zhong Yao Cai. 25(12): 888–890.